Ultra-Compact and Rugged Electrochemical Sensor for Monitoring Toxic Metals in Natural Water Sources

FINAL REPORT
JULY 24, 2018

Submitted by:

Mehdi Javanmard, Ph.D.
Assistant Professor

Robert Miskewitz, Ph.D.
Research Professor

Department of Electrical & Computer Engineering
Rutgers, The State University of New Jersey
98 Brett Rd.
Piscataway, NJ 08854

External Project Manager
Ali Maher, Ph.D.
Professor, CAIT Director

In Cooperation with
Rutgers, The State University of New Jersey
And
U.S. Department of Transportation
Federal Highway Administration

Disclaimer Statement

The contents of this report reflect the views of the authors, who are responsible for the facts and the accuracy of the information presented herein. This document is disseminated under the sponsorship of the Department of Transportation, University Transportation Centers Program, in the interest of information exchange. The U.S. Government assumes no liability for the contents or use thereof.

The Center for Advanced Infrastructure and Transportation (CAIT) is a National UTC Consortium led by Rutgers, The State University. Members of the consortium are the University of Delaware, Utah State University, Columbia University, New Jersey Institute of Technology, Princeton University, University of Texas at El Paso, Virginia Polytechnic Institute, and University of South Florida. The Center is funded by the U.S. Department of Transportation.

1. Report No.	2. Government Accession No.	3. Recipient's Catalog No.	
CAIT-UTC-NC41			
4. Title and Subtitle **Ultra-Compact and Rugged Electrochemical Sensor for Monitoring Toxic Metals in Natural Water Sources**		5. Report Date July 24, 2018 6. Performing Organization Code CAIT/Rutgers University	
7. Author(s) Azam Gholizadeh, Kelly Francisco, Robert Miskewitz, Ali Maher, Mehdi Javanmard		8. Performing Organization Report No. CAIT-UTC-NC41	
9. Performing Organization Name and Address Center for Advanced Infrastructure and Transportation Rutgers, The State University of New Jersey 100 Brett Road Piscataway, NJ 08854		10. Work Unit No. 11. Contract or Grant No. DTRT13-G-UTC28	
12. Sponsoring Agency Name and Address Center for Advanced Infrastructure and Transportation Rutgers, The State University of New Jersey 100 Brett Road Piscataway, NJ 08854		13. Type of Report and Period Covered Final Report 4/1/2016-11/15/2016 14. Sponsoring Agency Code	
15. Supplementary Notes U.S. Department of Transportation/OST-R 1200 New Jersey Avenue, SE Washington, DC 20590-0001			
16. Abstract The goal of phase I of this project was to provide a novel technology capable of assessment of sediment contamination in New York harbor. NY harbor is a major transportation and trade hub. The harbor contains 3-5 million cubic yards of sediment which is dredged out of the navigation channels per year. The sediment contains contamination. There is a demonstrated need for ultra-compact sensors which can perform in-situ detection of toxic compounds in complex environmental samples such as natural water sources and sedimentation. These sensors can be used to create accurate real-time mapping of panels of compounds both temporally and spatially. In Phase I of this project, we built a sample-to-answer system capable of detection of lead, copper, and chromium in unprocessed sediment. In Phase II, the proposed technology will be used to map spatial distribution across the harbor.			
17. Key Words Sensing, Environmental Monitoring, Toxic Compound Detection		18. Distribution Statement	
19. Security Classification (of this report) Unclassified	20. Security Classification (of this page) Unclassified	21. No. of Pages Total #24	22. Price

Form DOT F 1700.7 (8-69)

Acknowledgments

We would like to also acknowledge Masoud Janbaz and Kelly Francisco for helping with sediment collection.

Table of Contents

Table of Figures

DESCRIPTION OF THE PROBLEM

This project reports for the first time ever, to the best of our knowledge, an integrated on-chip sample-to-answer platform capable of qualitatively detecting lead ions directly in sediment samples. Sediment is one of the main sources of hazardous heavy metals in aquatic ecosystems. Rapid and real time detection of heavy metals in sediment is very crucial in the field of environmental monitoring. In-situ measurement of heavy metals with electrochemical sensors has been limited because of complicated pretreatment steps necessary to be performed on sediment. In this work, we present a sample-to-answer platform capable of on-chip sediment digestion and purification in conjunction with electrochemical quantification of lead ions. We have developed an integrated system consisting of a porous matrix for purification and extraction of Pb^{+2} on top of a graphene oxide thin film as the active sensing material. Although the proposed sensing platform is applicable to detection of a wide panel of toxic metals, we focused on platform validation using lead (Pb). First, the coated graphene oxide layer was characterized using electron microscopy, atomic force microscopy, and Raman. Then, we systematically studied optimization of various parameters affecting sensitivity and performance. Upon determining optimum experimental parameters, lead standard solution was analyzed with the optimized conditions. A linear working range with a detection limit of 4 ppb was established. After optimization of pretreatment parameters, the proposed electrochemical sensor was integrated with a 3D porous matrix for extraction and purification of lead ions for on-chip sample-to-answer analysis of complex sediment samples. The ability to detect lead directly in sediment samples with minimum volume of pretreatment agents and time makes this system a promising solution for in-situ detection of heavy metals for environmental monitoring.

APPROACH

One of the most dominant heavy metals present in the environment is lead as it is widely used in building materials, lead paints, and even lead-acid batteries. As a result of this overabundance in the environment, particularly in natural water sources and even drinking water, lead poisoning has resulted in many public health epidemics. Lead and other toxic metals that end up in natural water sources can often settle down to the bottom into the sediment. Contaminated sediment can get resuspended into natural water sources due to storms and transit of boats and vessels. The high concentration of lead in sediment (reported in the range of mg/kg[1]) when released into the water, poses risks to aquatic organisms and thus poses a serious public health problem. Based on reports, lead can damage the human nervous (especially children), respiratory, and reproductive systems[2]. Hence, the ability to rapidly screen sediment samples for lead is necessary to identify hot-spots of contaminated areas where remediation is necessary, to thus minimize the risk of re-suspension into natural water sources. To meet this requirement, there is a need for automated, portable, ultra-compact sensing devices capable of qualitatively identifying toxic metals directly in complex

environmental samples without the need for manhandling and sample preparation. Due to the detrimental health risks resulting from lead contamination, a variety of measurement methods have been developed. These methods include atomic absorption spectroscopy[3-6], inductive coupled plasma mass spectroscopy[7, 8], various optical [9-11] and electrochemical methods, which are primarily based on ion selective electrodes[12, 13] and stripping voltammetry[14-17]. Among these, because of high speed, high sensitivity, and portability, electrochemical stripping voltammetry is a promising method for tools capable of field measurements. Stripping voltammetry works well in purified buffers, however, to the best of our knowledge, to date, there have been no reports of electrochemical platforms capable of direct measurement of lead in sediment sample.

Electrochemical based sensors utilize a variety of electrode surface modifications for increasing sensitivity of lead detection. One example involves the reaction between tin and bismuth with lead and incorporation of these materials on the surface of the electrodes[18-21]. Also, a variety of other metal nanoparticles have been used, with the aim of increasing the surface area[22-25]. Other methods are based on using DNA enzymes[26, 27]. Additionally, graphene based nanomaterials due to their extraordinary electronic transport properties, large surface area, higher cathodic window thus avoiding reduction of hydrogen, and high electrocatalytic activities are another potential class of materials for electrode surface capable of sensitive lead detection[28-31]. Among them, graphene oxide, prepared through extensive chemical exfoliation of graphite flakes, has oxygen containing functional groups such as hydroxy, carboxy, epoxy, ether, diol and ketone, which are active sites for adsorbing heavy metals such as lead[21, 32].

Various methods allow for relatively easy deposition of graphene oxide (GO) thin films on top of electrode surfaces including drop casting[28-30, 33, 34], dip coating[35], Langmuir-Blodgett based deposition[36, 37], transfer via vacuum filtration,[38, 39] and spin coating[40-42]. The method used for deposition of GO is very important to control surface morphology, film uniformity, thickness and surface coverage. Among these methods, dip coating and drop casting often result in non-uniform deposition due to aggregation of GO sheets. Also drop casting GO suspension usually results in weak adhesion to electrode substrate. The rapid evaporation of the solvent during spin coating allows a more uniform surface with minimal wrinkling and increases the adhesion between the GO thin film and the electrode surface, which is critical during electrochemical reduction of GO.

Because of the ease and low cost for manufacturing, screen printed electrodes (SPE) have great utility as a disposable device. SPEs can be used for point-of-use testing in various applications such as industrial process monitoring, environmental monitoring, and food testing. Screen-printed electrodes combined with stripping voltammetry provide a promising solution for detection of heavy metals such as lead[43-45]. Various

lead sensors have been developed using SPEs. One example is disposable bismuth oxide modified SPE for detection of lead in the range of 20-300 ppb with a detection limit of 8 ppb[46]. In other works, SPEs modified by gold films displayed very highly linear behavior in the lead concentration range of 2-16 ppb with a detection limit of 0.5 ppb[47].

The key challenge to utilizing electrochemical methods for detecting heavy metals in complex matrices such as sediment, food, and soil at point-of-use is the requirement to perform a separate pretreatment step for extraction of ions and purification of sample. For lead, the ion extraction step is essential to convert all various chemical forms of lead to Pb^{2+} so that they can participate in the electrochemical reaction.

In this work, we present an ultra-compact sediment pretreatment module combined with a highly sensitive electrochemical graphene oxide sensor to detect lead in untreated sediment samples obtained directly from the environment. Our sediment pre-treatment module consists of a cellulose sponge, which serves as a membrane between the sediment and the active site of the sensor. Sponges have demonstrated significant ability to adsorb contamination,[48] thus making them a suitable choice of material for the porous membrane. The porous membrane adsorbs contamination of sediment preventing direct contact between solid sediment and the active graphene oxide site. Moreover, lead ions easily penetrate through the cellulose sponge membrane and thus pure solution reaches the graphene oxide surface. An additional benefit to this approach is that this set up minimizes the required acidic pretreatment to microliter levels.

Moreover, we selectively spin-coated GO uniformly onto a screen printed gold working electrode and investigated the performance of the sensor over a wide range of parameters to optimize the performance. Gold screen-printed electrodes are high in conductivity and exhibit excellent performance of stripping voltammetry and are thus chosen as the working electrode for deposition of GO[49-51]. The surface morphology and chemical characterization of the GO film was done using scanning electron microscopy (SEM), atomic force microscopy (AFM) and Raman Spectroscopy. The analytical parameters affecting the sensor performance and the thin film fabrication were studied in terms of concentration of GO solution during spin coating, the effect of GO reduction, the supporting electrolyte, square wave anodic stripping voltammetry (SWASV) parameters such as deposition time, frequency, and pulse height. The reliability of the electrode in response to high concentrations of lead was also investigated to ensure the capacity of lead adsorption on the surface of the electrode. Furthermore, the effect of water extracted from sediment on the supporting electrolyte was investigated both with and without adding acetate buffer solution in the range of 0 ppb to 20 ppm lead standard. This was then used to quantify the amount of lead present in digested sediment samples collected from the environment.

METHODOLOGY

Reagents and Instrumentation. Pb (II) standard solution was prepared using lead nitrate stock standard solution in various supporting electrolytes. GO solutions were prepared from standard stock solution of 2 $mgmL^{-1}$ (Sigma Aldrich, MO, USA). To avoid aggregation of GO sheets, each solution underwent ultrasonication and centrifugation immediately prior to spin coating.

A potentiostat (Gamry 600, Gamry Instruments, Pennsylvania, USA) was used to perform electrochemical measurements. Screen printed electrodes with gold working (5 mm) and counter electrodes and an Ag/AgCl reference electrode was purchased from USA Metrohm. All electrochemical experiments were conducted in ambient conditions, except for reduction of GO which underwent purging using high purity nitrogen. Ambient conditions were chosen to ensure that platform is fully compatible with field-use.

The morphology of graphene oxide was characterized using field-emission scanning electron microscopy (SEM) (Zeiss Leo Field Emission SEM, Carl Zeiss) and atomic force microscopy (AFM) (Digital Instruments Nanoscope IV). The atomic force microscope was operated in tapping mode using standard cantilevers with a spring constant of 40 $N\ m^{-1}$ and a tip curvature of 10 nm. FT-Raman spectra (Horiba Johin-Yvon Micro Raman Spectrometer, 532 nm excitation laser) were recorded to characterize graphene oxide substrates.

The sediment sample was collected in the Arthur Kill at the mouth of Morse's Creek in Linden NJ. It was collected using a Smith Mack box corer lowered from a boat in a depth of approximately 6 feet of water. The sample consisted of a composite of the sediments from 0 to 25 cm below the sediment water interface.

Sensor Fabrication. The compact sensor system developed herein comprises two main components, (i) a modified electrochemical sensor with GO, and (ii) a pretreatment column consisting of a cellulose sponge. The steps required to modify the gold working electrode with a spin coated layer of GO are shown in figure 1. First a thin PDMS membrane is spin coated onto the screen printed electrode. This step is performed for two purposes. First, the PDMS protects the counter and reference electrode from electrical shortage during deposition of GO solution. Second, the PDMS layer serves as a scaffold to structurally support the pretreatment column. To prepare the PDMS mask, a 10:1 ratio of Sylgard PDMS with respect to the curing agent was mixed together thoroughly. After degassing and removing bubbles, the PDMS thin film was coated in a two-step process with 500 rpm for 5 seconds and 4000 rpm for 30 seconds on the SPE substrate. After curing in 80 °C for 1 hour, an approximately 20 µm thick PDMS membrane is formed on top of the electrodes. The film of PDMS on top of the working electrode was manually removed and then the solution of GO was deposited on top of the working electrode with the same coating parameters. Afterwards, the

PDMS membrane was removed from the counter and reference electrodes and the contact pads. The substrate is then washed with isopropyl alcohol to ensure removal of possible residue of PDMS from the surface of the electrodes.

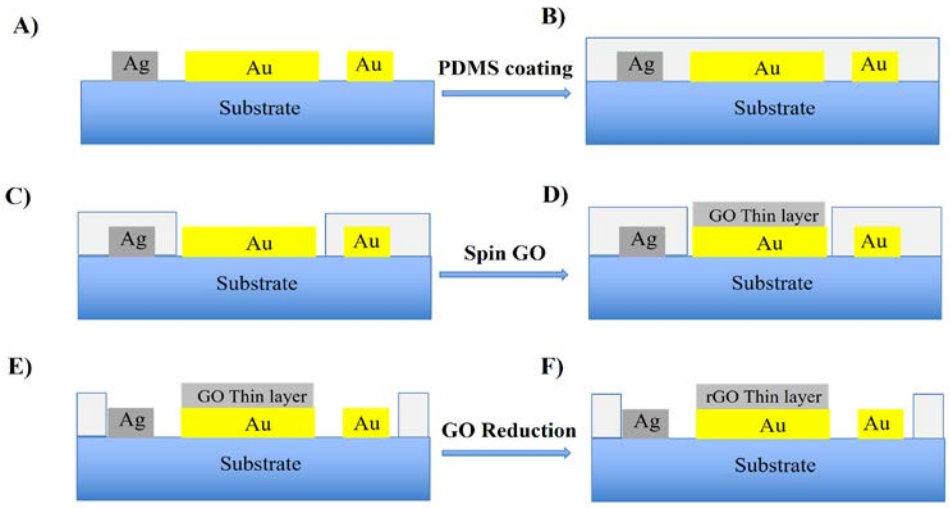

Figure 1: Fabrication process for spin coated GO thin film on Gold SPE electrode.

To compare the performance of the GO sensor with reduced graphene oxide (rGO), GO was reduced electrochemically using cyclic voltammetry between -1.6 to 0 V in 0.3 M acetate buffer (pH 5) with a scan rate of 25 mV s^{-1} for 30 scans under continuous Nitrogen gas (N_2) purging. We used platinum as the choice of the counter electrode material to avoid damage during the reduction process.

The pretreatment column is assembled with a 5 mm PDMS layer. To connect column to sensor active site, an 8 mm hole is punched through the PDMS layer. An Eppendorf tube is used as the pretreatment column. The pretreatment column adheres on top of the hole with glue. A sponge (2 mm high) is located between the sediment sample and the hole inside the column. Syringe tips are used for inserting the required agents for pretreatment. Figure 2 shows the schematic and an image of the fabricated compact sensor set up. The pretreatment column is assembled with a 5 mm thickness PDMS layer. An Eppendorf tube is used as pretreatment column. A sponge is located between sediment sample and the hole inside the column. The pretreatment column is connected on top of sensor with glue through the 8 mm hole punced on PDMS layer. Syringe tips are used for inserting required agents for pretreatment inside the setup.

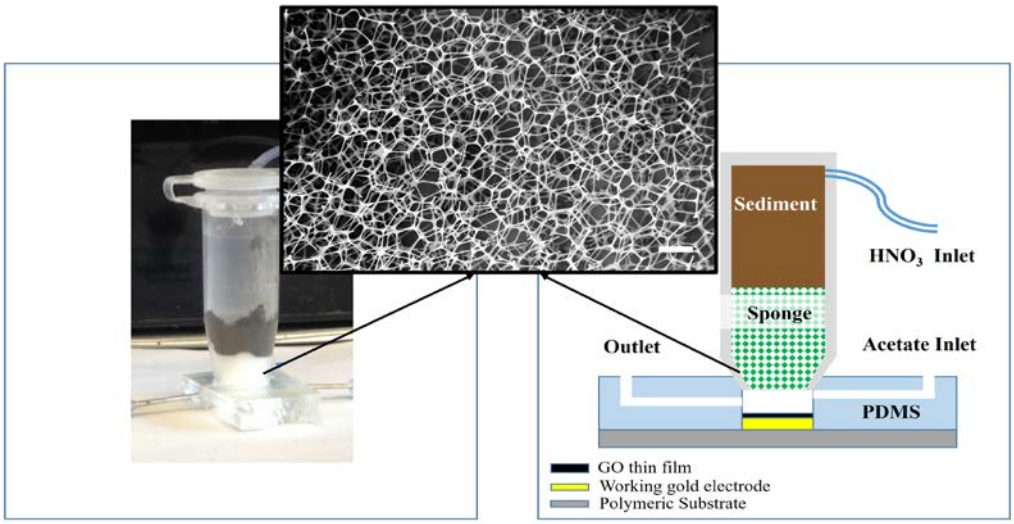

Figure 2: The image of compact electrochemical lead sensor. The schematic of set up design and SEM of cellulose sponge, scale bar is 200 µm.

FINDINGS

GO thin film characterization and optimization. The morphology of the graphene oxide film was studied using AFM and SEM. Raman spectroscopy was used to determine the extent of reduction of the graphene oxide layer. Figure 3A shows the SEM image taken from a spin-coated 2 mg mL^{-1} graphene oxide layer on the surface of the working gold electrode. This illustrates 50 µm of a graphene oxide large sheet that can form a uniform layer in most areas despite the roughness (micron scale features) of the gold electrode surface. In comparison to drop-casting which is typically used in electrochemically modified electrodes, this method provides more reproducibility and enables formation of much larger areas of GO films without agglomeration. Figure 3B shows two dimensional AFM images of a graphene oxide flake with wrinkles. These wrinkles can be produced during vaporization of the solvent during spin coating. From the height profile, the film can be approximated to have a thickness of 1.5 nm that is typical amount for GO sheet (supporting information S1).

We tested and characterized both graphene oxide and reduced graphene oxide films to determine which of the two has better performance in detection of lead. Thus, we used electrochemical reduction of the GO films, and the quality of reduction was investigated using Raman spectroscopy. Figure 3C shows the Raman spectrum of graphene oxide and the electrochemically reduced film. The most important features in the Raman spectra for assessment of graphene oxide reduction are the G and D peaks. These peaks arise from vibration of sp^2 carbon and appear around 1600 and 1340 cm^{-1} respectively.

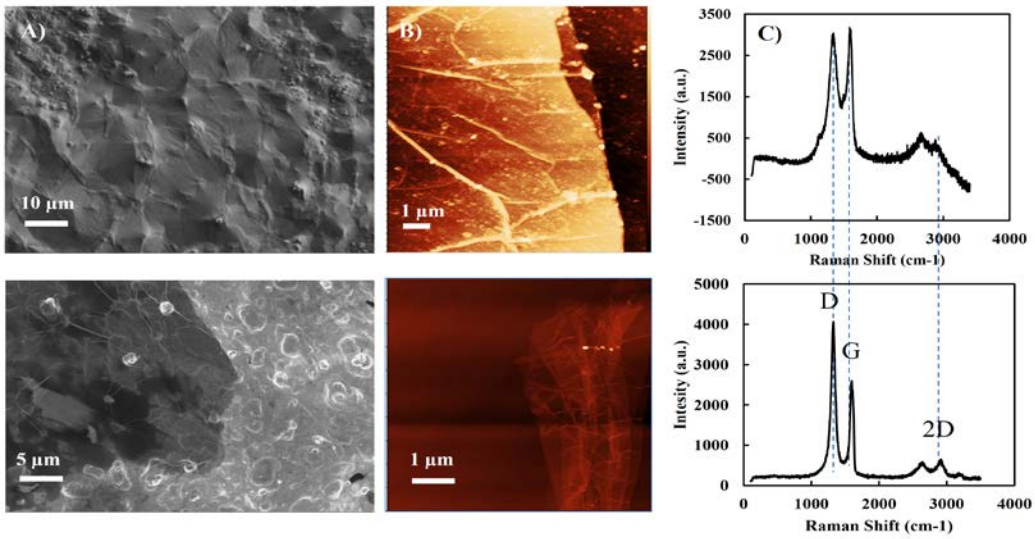

Figure 3: A) SEM image of GO thin film on gold electrode surface, B) 2 and 3D Atomic force microscopy images on glass slide. C) Raman spectrum of GO (top), and rGO (bottom) image.

The overtone of the D peak appearing around 2700 cm^{-1} is called the 2D peak. Unlike mechanically exfoliated graphene, the GO 2D band usually has low intensity because it is more disordered. Therefore, the peaks that can be used to distinguish between GO and rGO are the G and D peaks and their ratio. Also the G peak of GO and rGO with respect to graphene and graphite gets shifted into higher frequencies (1600 cm^{-1}) because of defects in the film. This ratio exhibited a significant increase compare to GO (from 0.98 to 1.57). This shows restoration of sp^2 carbon and a decrease in the average size of sp^2 domains after electrochemical reduction of GO. The increasing in intensity of the 2D peak also suggests better graphitization[52].In order to explore the activation of the modified working electrode, the electrochemical performance was evaluated using differential pulse voltammetry (DPV). As shown in Figure 4A and 4B, an increase in concentration of spin coated GO solution increases the current intensity in response to 10 ppm of lead standard solution. Also, the current intensity exhibited from GO electrodes is higher compared to that of rGO, likely because the interaction between oxygen functionalized groups with lead ions. The data suggest that among the different working electrodes we fabricated, the spin coated GO film (concentration of 2 mg mL^{-1}) exhibits the fastest electron transfer rate for lead ions.

We electrochemically characterize the electrode film using an inner sphere redox probe, potassium ferrocyanide. Figure 4C shows representative data of cyclic voltammogram obtained for an unmodified gold SPE and also various spin coated GO films. The gold SPE exhibits a pair of well-defined redox peaks, with a peak-to-peak separation of 78 mV. The peak separation can be used to determine hetero-electron transfer (HET) rate. In the case of linear mass transfer, smaller separation of the peaks indicates increasing reversibility and higher HET rate. Electrochemical characterization of the GO thin films exhibits an

increasing peak separation with respect to the concentration of GO suspension. The peak separations for GO solution concentrations between 0.2-2 mg mL^{-1}, ranges from 82 to 176 mV.

The electrochemical response of graphene based electrodes towards the ferrocyanide redox probe is influenced by the density of states near the fermi level and more significantly by surface morphology and the presence of oxygenated species[53].

To further characterize the electrochemical performance of the device, we also performed electrochemical impedance spectroscopy (EIS). Nyquist plot for the electrodes are shown in figure 4D. The shape of plot depends on the applied voltage. All impedances were biased to the redox voltage of ferrocyanide, which was 0.115 V. The charge transfer resistance (R_{ct}) values (based on real part of the impedance in EIS measurements) are in agreement with the cyclic voltammograms response. With increasing GO concentration HET decreases and R_{ct} increases to higher values. Also, 2 mg mL^{-1} GO shows higher (constant phase element) CPE, indicating a rougher surface in this case.

The comparison of results from GO and rGO show the oxygen groups on the surface of GO, as expected, play an important role in detection of lead ions. Although the electron transfer of GO in ferrocyanide is lower compared to normal SPEs and rGO electrodes, a higher current response with respect to lead ions is observed.

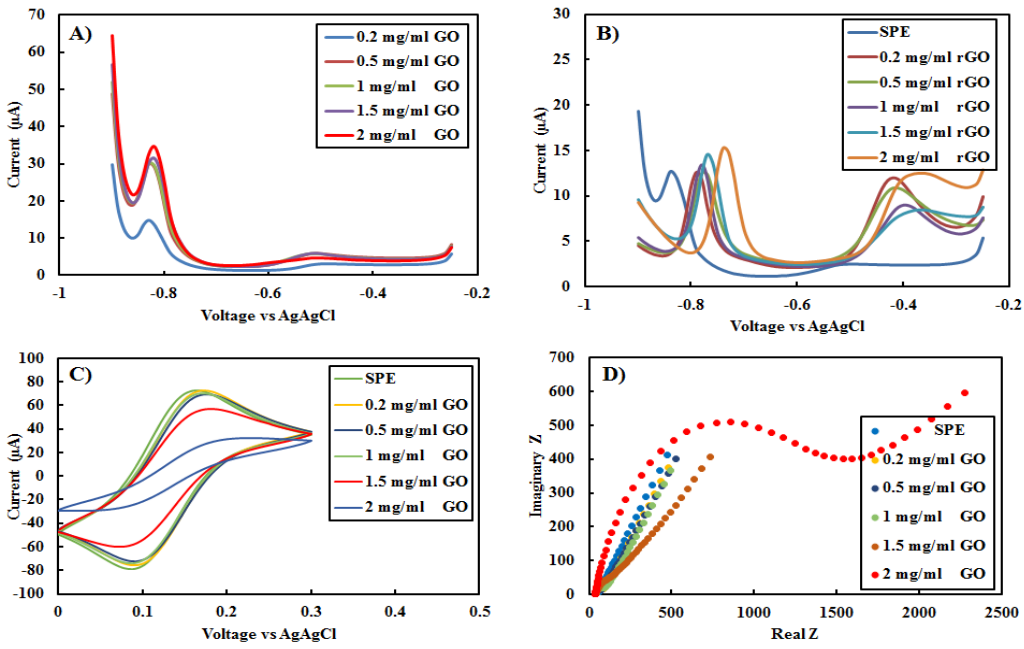

Figure 4: A, B) Differential pulse voltammograms obtained for different GO and rGO concentration electrodes respectively. DPV performed from -0.9 to -0.2 V, with step size 10 and pulse size 50 mV in 10 ppm lead in 0.1 M acetate buffer (pH 5). C) Cyclic voltammograms of different GO concentrations electrodes in 5 mM K3Fe(CN)6 in 0.1 M KCl. Scan rate is 20 mvs-1. D) Electrochemical impedance curves in 5 mM K3Fe(CN)6/K4Fe(CN)6, 0.1 M KCl. The spectra were taken at 0.1 Hz to 1 MHz, 0.115 v dc vs Ag/AgCl.

Various electrolytes were tested to find the optimal buffer for lead analysis. Among them, HCl and KCl react very aggressively with the electrodes and destroy them. Also HNO_3 has a large peak in -0.4 V that covers up the lead peak, especially in the low concentration range, and makes the detection of lead impossible. Between PBS (pH 7) and acetate (pH 5), acetate has better performance and lower background current and as a result, 0.1 M acetate buffer with pH 5 was selected for measurement of lead concentrations.

Sensor Response in Lead Standard. The cyclic voltammogram (CV) of the electrodes was obtained using a lead standard solution of 100 ppm at a scan rate of 50 mV s^{-1} (figure S2A). A redox peak corresponding to the lead ion appeared in -0.68, -0.74 V. Based on the difference between the cathodic and anodic peak location, the electrode shows a quasi-reversible response towards lead ions. When performing up to 20 scans, the peak location and intensity, after the second scan remains consistent, showing the stability of the electrode surface for lead ions even in the presence of very high concentrations of lead.

Figure S2B shows the differential pulse voltammetry (DPV) peak increasing with the concentration of lead. This gives us confidence that this peak results from the presence of lead ions and not nitrate which is in the lead standard solution.

As SWASV (Square Wave Anodic Stripping Voltammetry) has proven to be a powerful electrochemical method for sensing heavy metal ions, we selected this as our electrochemical method in this work. First, we studied the effect of the most important SWASV parameters, namely accumulation potential, time, the number of pulses, and the applied frequency.

As shown in figure 5, when we ramped up the pulse amplitude until 50 mV, the peak current plateaus and afterwards it stays steady as the pulse amplitude is increased. Also, the peak current response of GO SPE electrode was measured at different frequencies. After 30 Hz, the peak splits into two peaks so 20 Hz is selected for the measurements. The peak current gradually increased with accumulation time until 240 s. The maximum peak current was obtained in deposition voltage of -1 V. However, because of the over-potential involved during reduction of hydrogen on the surface of the electrodes, lower voltages are desirable for the purpose of long-term usage. As our final goal is dipping sensor in bucket of sediment and doing in situ measurement, all SWASV analysis have been done in stationary and ambient condition. The response in this condition shows enough sensitivity for low concentration range of lead detection.

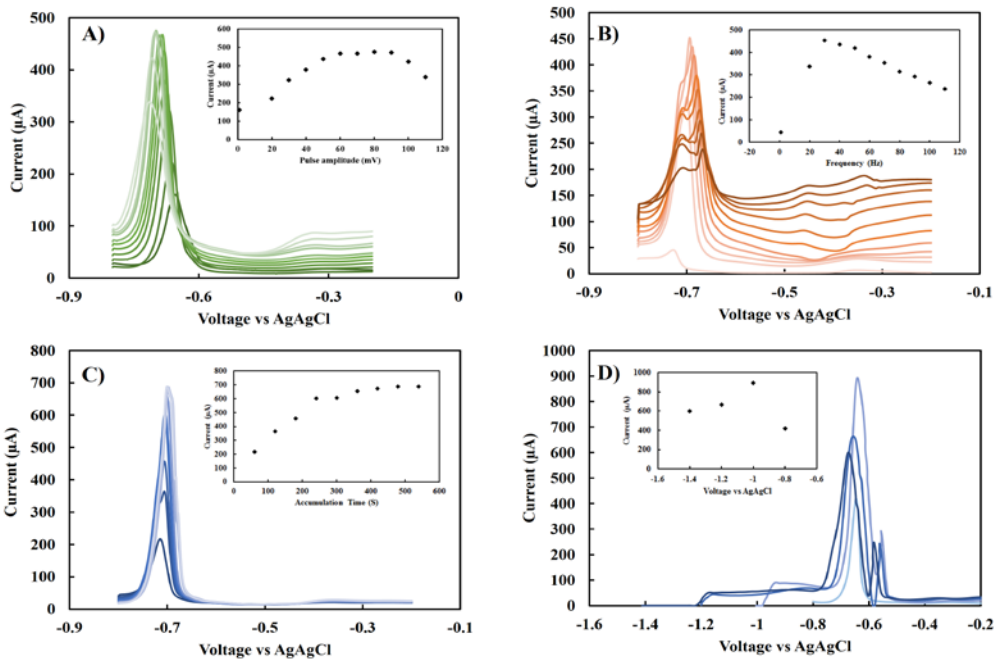

Figure 5: A, B, C,D) Square wave anodic stripping voltammograms of different pulse amplitude, frequency, accumulation time and accumulation voltage respectively. Lead concentration was used is 20 ppm in 0.1 M acetate buffer (pH 5).

After calibration of SWASV parameters, the analytical performance of the lead GO-SPE was explored by SWASV. Figure 6A, B show SWASV measurements conducted from -0.85 to -0.4 V vs Ag/AgCl in acetate buffer (pH 5) for a wide range of lead ion concentrations (2 ppb-20 ppm). The peak current appeared between -0.75 and -0.66 V. At low concentration levels, which is the range of interest for sediment analysis, the corresponding peak appeared at -0.75 V. The data has been corrected based on base line current. Figure 6C, D shows the calibration curves, indicating the presence of two linear ranges. To calculate the sensitivity of the sensor towards lead ions, the effective surface area was obtained using the Randles-Sevcik equation. Based on the slope of the current verses the square root of the scan rate in 5 mM $K_3Fe(CN)_6$ in 0.1 M KCl, the active surface area for spin coated 2 mg mL^{-1} of GO on top of the SPGE is equal to 0.025 cm^2. On the basis of this area, the fabricated sensor shows a sensitivity of 1.73 µA ppb^{-1} cm^{-2} in low and 1.9 µA ppb^{-1} cm^{-2} in the high concentration range with a low detection limit of 4 ppb. The steady peaks in very high concentration levels indicates that the surface of GO is not saturated so we can assume the bond between oxygen functional group on the surface of GO with lead ions is reversible and this sensor can be reused multiple times.

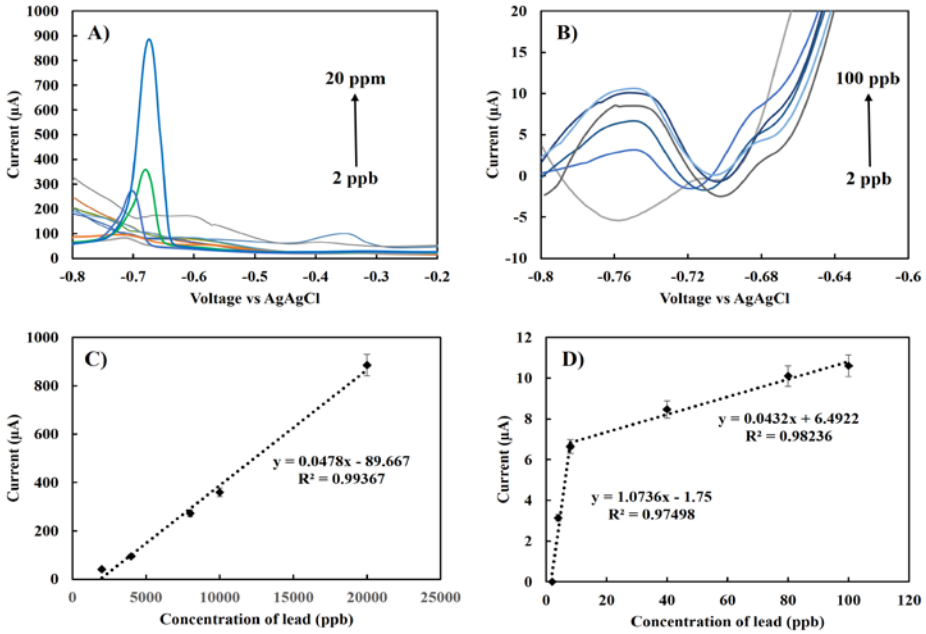

Figure 6: A, B) Square wave anodic stripping voltammogram of different range of lead standard solution in acetate buffer (0-20 ppm). Pulse size is 50 mV, frequency 20 Hz, accumulation time 240 s. C, D) Calibration curve for different concentration range of lead standard solutions.

Lead Detection in Sediment Samples. After testing the performance of the fabricated sensor on lead standard solutions, we turned our attention to characterize the ability of the sensor to detect lead concentrations in contaminated complex environmental samples.

Spiked Sediment Samples: First, we tested the sensor's ability to detect lead in water extracted from contaminated sediment. Before testing for basal levels of lead in processed environmental sample, we tested environmental samples spiked with lead to study the effect of the matrix on the sensor. First, 10 µl of standard lead solution was spiked into untreated water extracted from the sediment, but no peak was observed, even despite adding high concentrations of lead. To resolve this issue, we added acetate buffer into the matrix. Figure S3 shows the SWASV response of the sensor in the range of 2 ppb-20 ppm, spiked at a 1:1 ratio of standard solution in acetate in water, which was extracted by centrifuge from the sediment samples. The magnitude of the redox current generated for 20 ppm is four times lower than lead standard in purified acetate buffer. The results show that the water extracted from the sediment has a significant effect on inhibiting the lead redox currents. The inset shows a range of 2-1000 ppb, which is the range of interest for lead in sediment samples. Based on the data obtained, we concluded that the presence of acetate buffer is crucial to detection of lead in sediment samples.

Off-Chip Sample Preparation: For measurement of basal concentrations of lead ions adsorbed to sediment, the sediment must first be digested with nitric acid to convert the various types of lead compounds to Pb

(II). 1 gr Sediment (0.9 gr after water evaporation) was dispersed in nitric acid and then filtered using Whatman filter paper (Figure 7A). Ultrasound was used for 1 hour in 60º C in three different concentration of nitric acid. Figure 7B shows the SWASV peaks for lead in a 1:1 ratio of digested sediment in nitric acid/acetate buffer. Among various concentrations, 0.1 M nitric acid was chosen based on peak current intensity and the need for a less aggressive solution on the electrode surface.

To quantify the amount of lead, SWASV was performed for different lead standard solutions in the same electrolyte composition used for digestion (1:1 ratio 0.1 M nitric acid/acetate buffer). The results are shown in figure 7C. Finally, we performed the digestion without using ultrasound in room temperature. Figure 7D shows the average result for three different measurement of samples with RSD 10%. The peak intensity is significantly higher than before, which was unexpected, however this phenomenon can be explained with the concept of adding residues of sediment during ultrasonication that can passivate the surface of the electrode. Based on the calibration data, the amount of lead in this sample is approximately 21±2 mg kg^{-1} of sediment, which is comparable with the range of lead in sediment reported in previous studies[1].

Integration of Sample Preparation with Sensing Chip. After determining the appropriate reagents and conditions for sediment digestion, lead extraction, and purification, we focused our efforts on miniaturization and integration of sample-preparation on-chip.

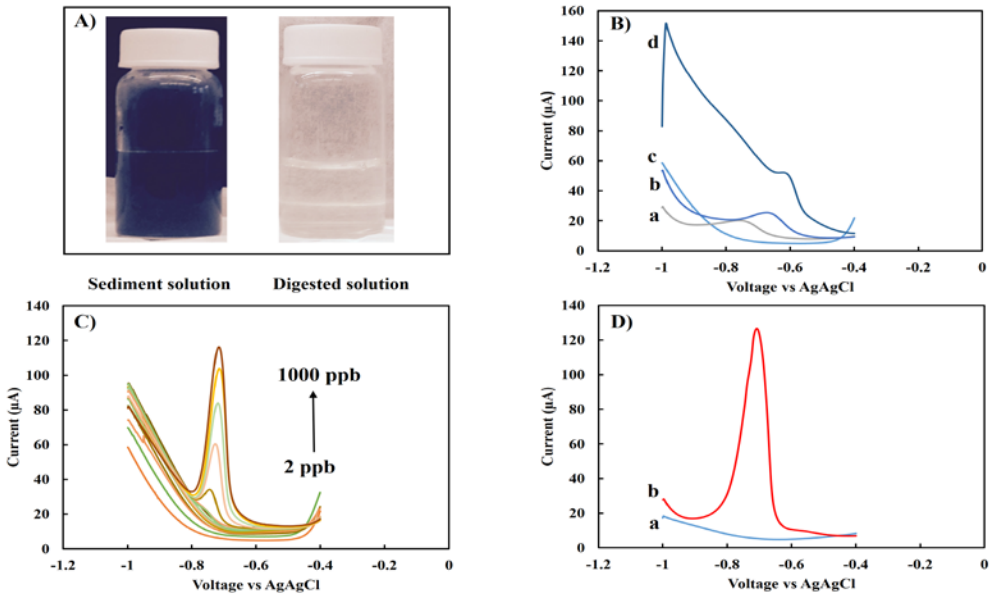

Figure 7: A) Solution of sediment in nitric acid before and after filtration. B) Effect of concentration of nitric acid using ultrasound digestion in 60 degrees a) digested in 0.1 M nitric acid, b) 0.2 M nitric acid. c) blank buffer solution 0.2 M nitric acid/acetate buffer, d) 0.3 M nitric acid C) SWASV peaks for different concentration of lead standard solution in 1:1 nitric acid and acetate buffer. D) SWASV peaks for a) 0.1 M nitric acid/acetate buffer blank, b) digested lead in 0.1 M nitric acid/acetate buffer.

The filter paper and cellulose sponge was assembled on top of the GO sensor (figures 8B, C). Then amount of 0.1 grams sediment was injected onto the surface of the cellulose sponge (figure 8D). Nitric acid (0.1 M) was manually injected onto the sediment, thus extracting lead ions, which then diffused to the acetate buffer below the membrane. This allowed for the lead ions to be suspended in an optimal buffer (acetate) for detection purposes. The lead ions continue to diffuse further until they reach the GO sensor and get detected. Figure 8D shows the average result of SWASV measurement using this integrated sample-to-answer set up. This initial result was very encouraging showing that integrated sample preparation was feasible, however, we moved towards an integrated fluidic system to minimize the need for manhandling and manual injection of reagents.

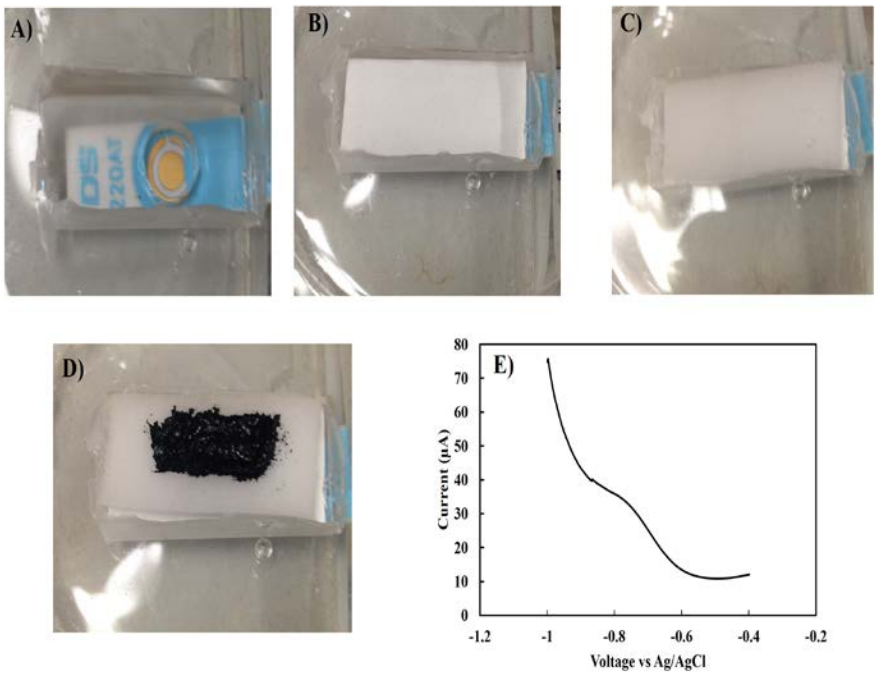

Figure 8: A) GO thin film on SPE electrode with PDMS membrane, B) adding filter paper C) adding sponge, D) adding sediment sample, E) the SWAVS response of sensor set up.

As a result, the design was modified to incorporate precise microfluidic control to enable automation. To allow sufficient time for sediment digestion and minimize user manhandling of reagents, a column was used to introduce sediment and nitric acid to the device (figure 9A). In addition, this design effectively decreases the volume of nitric acid (which is hazardous) required to the microliter range. Moreover, separate inlet and outlets added to the set up that allow user to more precise control the ratio of reagents. They are located as follows: The nitric acid inlet is located at the top of the column. The outlet is located in middle of the PDMS hole. The inlet of the acetate buffer is located on top of the hole. With this design, reagents

are introduced at a (1:1) ratio to help obtain reproducible results comparable to those obtained from calibration experiments. Figure 9B shows the result of the lead measurement obtained with this set up for 0.45 grams of dried sediment. Results are compared with traditional pretreatment methods revealing 80 percent peak recovery (figure 9 C,D) .

Here, we introduced an integrated sample-to-answer platform capable of analyzing heavy metal ions in complex samples like sediment. The results demonstrate that this approach shows promise for an in-situ platform capable of continuously monitoring heavy metal concentrations complex environmental samples such as sediment in natural water sources. Though we focused on sediment, we emphasize the applicability of this platform to perform sample-to-answer analysis in other complex matrices such as soil and food 54, 55. The approach presented in this manuscript use a considerably shorter time for digestion sediment compared to off-chip pretreatment methods. Further improvement can be made to the design presented here by incorporating a closed-feedback loop based input set up. This set up allows the sediment exposes several times to the same volume of nitric acid, thus dramatically increasing the exposure time.

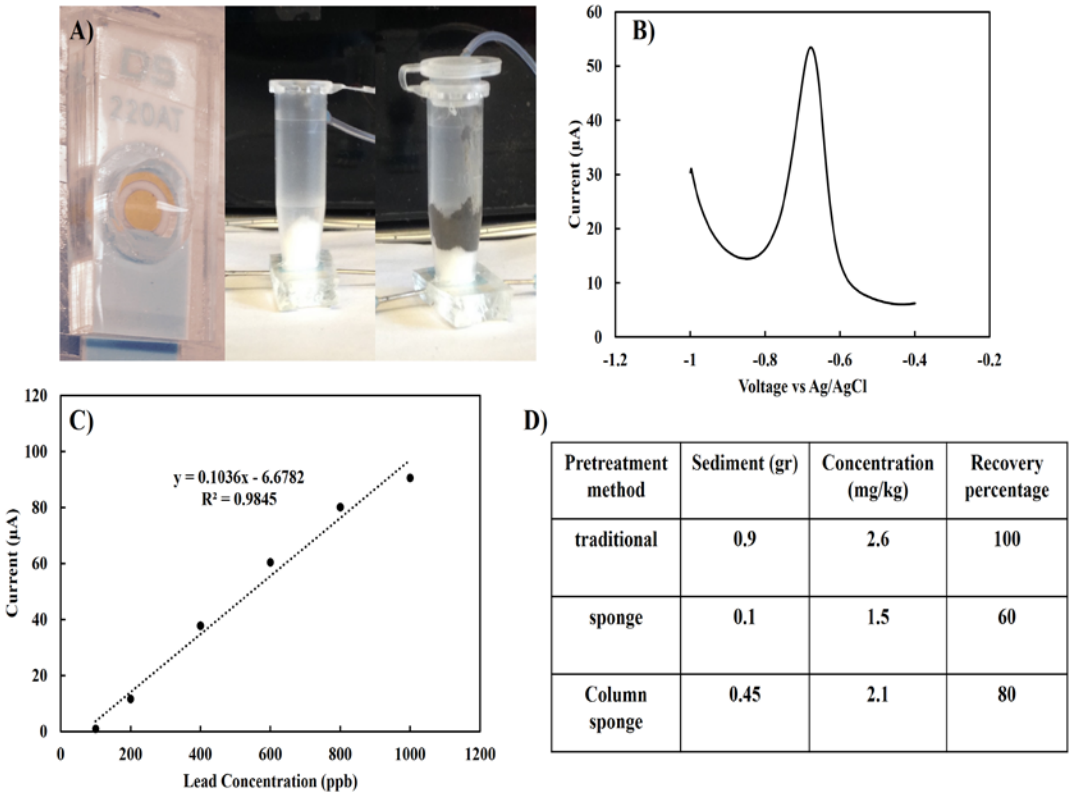

Pretreatment method	Sediment (gr)	Concentration (mg/kg)	Recovery percentage
traditional	0.9	2.6	100
sponge	0.1	1.5	60
Column sponge	0.45	2.1	80

Figure 9: A) column based pretreatment set up, B) SWAVS response of column based compact electrochemical lead sensor, C) Calibration curve for (1:1) nitric acid: acetate after baseline correction, D) comparing results for different pretreatment approaches based on calibration curve.

CONCLUSIONS

An integrated miniaturized, sample-to-answer electrochemical sensor system based on graphene oxide has been developed, calibrated and tested in both standard lead solutions and complex sediment samples. This work shows that square wave stripping voltammetry based electrochemical detection of lead is a promising analytical tool for monitoring heavy metals in complex matrices, and this work can fill the current gap for on-line heavy metal monitoring electrochemical based system in natural water sources.

In this study, we utilized the outstanding electrochemical properties of graphene oxide thin films with respect to lead ions to fabricate a label-free method for measurement of low abundance toxic metals in sediment samples. We systematically optimized modification of the electrodes and the electrochemical measurement parameters in buffer solution, which allows us to measure the presence lead in low abundance. The sensitivity of the sensor was 1.73 μA ppb^{-1} cm^{-2} in the range of 0-100 ppb and 1.9 μA ppb^{-1} cm^{-2} in 100 ppb to 20 ppm with a low detection limit of 4 ppb. We tested the performance of the sensor both in environmental samples spiked with lead (to test the effect of the matrix), and we also tested basal levels of lead in digested sediment. Then we introduced a portable pretreatment set-up as an ultra-compact fully nitrated sample-to-answer system. This sensor showed the ability to quantify low abundance heavy metals in sediment. We envision miniaturizing the potentiostat used to readout the electrochemical sensor into a portable instrument resulting in a low cost rapid field analyzer capable of sample-to-answer analysis simultaneously with collection of sediment, which can be an alternative to expensive and time consuming methods such as atomic adsorption and Inductively Coupled Plasma Mass Spectrometry.

RECOMMENDATIONS

Now that the initial sensing platform has been built and fabricated, we will direct our efforts to integrating this with a cone penetrometer and performing spatio-temporal mapping experiments in the NY Harbor.

REFERENCES

1. Zhang, Z.; Li, M.; Chen, W.; Zhu, S.; Liu, N.; Zhu, L., Immobilization of lead and cadmium from aqueous solution and contaminated sediment using nano-hydroxyapatite. *Environmental Pollution* **2010,** *158* (2), 514-519.
2. ATSDR, U., Toxicological profile for lead (Atlanta, GA: US Department of Health and Human Services, Agency for Toxic Substances and Disease Registry (ATSDR), Public Health Service). *US EPA (2006) Air quality criteria for lead* **2007**.
3. Ghaedi, M.; Shokrollahi, A.; Niknam, K.; Niknam, E.; Derki, S.; Soylak, M., A cloud point extraction procedure for preconcentration/flame atomic absorption spectrometric determination of silver, zinc, and lead at subtrace levels in environmental samples. *Journal of AOAC International* **2009,** *92* (3), 907-913.
4. Citak, D.; Tuzen, M., Cloud point extraction of copper, lead, cadmium, and iron using 2, 6-diamino-4-phenyl-1, 3, 5-triazine and nonionic surfactant, and their flame atomic absorption

spectrometric determination in water and canned food samples. *Journal of AOAC International* **2012,** *95* (4), 1170-1175.
5. Soylak, M.; Yilmaz, E.; Ghaedi, M.; Montazerozohori, M.; Sheibani, M., Cloud point extraction and flame atomic absorption spectrometry determination of lead (II) in environmental and food samples. *Journal of AOAC International* **2012,** *95* (6), 1797-1802.
6. Sitko, R.; Janik, P.; Feist, B.; Talik, E.; Gagor, A., Suspended aminosilanized graphene oxide nanosheets for selective preconcentration of lead ions and ultrasensitive determination by electrothermal atomic absorption spectrometry. *ACS applied materials & interfaces* **2014,** *6* (22), 20144-20153.
7. Caroli, S.; Forte, G.; Iamiceli, A.; Galoppi, B., Determination of essential and potentially toxic trace elements in honey by inductively coupled plasma-based techniques. *Talanta* **1999,** *50* (2), 327-336.
8. Munro, S.; Ebdon, L.; McWeeny, D. J., Application of inductively coupled plasma mass spectrometry (ICP-MS) for trace metal determination in foods. *Journal of Analytical Atomic Spectrometry* **1986,** *1* (3), 211-219.
9. Zhao, L.; Zhong, S.; Fang, K.; Qian, Z.; Chen, J., Determination of cadmium (II), cobalt (II), nickel (II), lead (II), zinc (II), and copper (II) in water samples using dual-cloud point extraction and inductively coupled plasma emission spectrometry. *Journal of hazardous materials* **2012,** *239*, 206-212.
10. Pelossof, G.; Tel-Vered, R.; Willner, I., Amplified surface plasmon resonance and electrochemical detection of Pb2+ ions using the Pb2+-dependent DNAzyme and hemin/G-quadruplex as a label. *Analytical chemistry* **2012,** *84* (8), 3703-3709.
11. Choudhary, R.; Patra, S.; Madhuri, R.; Sharma, P. K., Equipment-Free, Single-Step, Rapid,"On-Site" Kit for Visual Detection of Lead Ions in Soil, Water, Bacteria, Live Cells, and Solid Fruits Using Fluorescent Cube-Shaped Nitrogen-Doped Carbon Dots. *ACS Sustainable Chemistry & Engineering* **2016,** *4* (10), 5606-5617.
12. Malon, A.; Vigassy, T.; Bakker, E.; Pretsch, E., Potentiometry at trace levels in confined samples: ion-selective electrodes with subfemtomole detection limits. *Journal of the American Chemical Society* **2006,** *128* (25), 8154-8155.
13. Huang, M.-R.; Ding, Y.-B.; Li, X.-G.; Liu, Y.; Xi, K.; Gao, C.-L.; Kumar, R. V., Synthesis of semiconducting polymer microparticles as solid ionophore with abundant complexing sites for long-life Pb (II) sensors. *ACS applied materials & interfaces* **2014,** *6* (24), 22096-22107.
14. Prabakar, S. R.; Sakthivel, C.; Narayanan, S. S., Hg (II) immobilized MWCNT graphite electrode for the anodic stripping voltammetric determination of lead and cadmium. *Talanta* **2011,** *85* (1), 290-297.
15. Li, J.; Guo, S.; Zhai, Y.; Wang, E., High-sensitivity determination of lead and cadmium based on the Nafion-graphene composite film. *Analytica chimica acta* **2009,** *649* (2), 196-201.
16. Armstrong, K. C.; Tatum, C. E.; Dansby-Sparks, R. N.; Chambers, J. Q.; Xue, Z.-L., Individual and simultaneous determination of lead, cadmium, and zinc by anodic stripping voltammetry at a bismuth bulk electrode. *Talanta* **2010,** *82* (2), 675-680.
17. Stauber, J.; Florence, T., The determination of trace metals in sweat by anodic stripping voltammetry. *Science of the Total Environment* **1987,** *60*, 263-271.
18. Wang, Z.; Liu, G.; Zhang, L.; Wang, H., A bismuth modified hybrid binder carbon paste electrode for electrochemical stripping detection of trace heavy metals in soil. *Int. J. Electrochem. Sci* **2012,** *7*, 12326-12339.
19. Kokkinos, C.; Economou, A.; Raptis, I.; Speliotis, T., Disposable lithographically fabricated bismuth microelectrode arrays for stripping voltammetric detection of trace metals. *Electrochemistry Communications* **2011,** *13* (5), 391-395.
20. Lee, G.-J.; Lee, H.-M.; Rhee, C.-K., Bismuth nano-powder electrode for trace analysis of heavy metals using anodic stripping voltammetry. *Electrochemistry Communications* **2007,** *9* (10), 2514-2518.

21. Wei, Y.; Gao, C.; Meng, F.-L.; Li, H.-H.; Wang, L.; Liu, J.-H.; Huang, X.-J., SnO2/reduced graphene oxide nanocomposite for the simultaneous electrochemical detection of cadmium (II), lead (II), copper (II), and mercury (II): an interesting favorable mutual interference. *The Journal of Physical Chemistry C* **2011,** *116* (1), 1034-1041.
22. Zhu, L.; Xu, L.; Huang, B.; Jia, N.; Tan, L.; Yao, S., Simultaneous determination of Cd (II) and Pb (II) using square wave anodic stripping voltammetry at a gold nanoparticle-graphene-cysteine composite modified bismuth film electrode. *Electrochimica Acta* **2014,** *115*, 471-477.
23. Mahmoudian, M.; Alias, Y.; Basirun, W.; Woi, P. M.; Sookhakian, M.; Jamali-Sheini, F., Synthesis and characterization of Fe 3 O 4 rose like and spherical/reduced graphene oxide nanosheet composites for lead (II) sensor. *Electrochimica Acta* **2015,** *169*, 126-133.
24. Lee, P. M.; Chen, Z.; Li, L.; Liu, E., Reduced graphene oxide decorated with tin nanoparticles through electrodeposition for simultaneous determination of trace heavy metals. *Electrochimica Acta* **2015,** *174*, 207-214.
25. Tang, S.; Tong, P.; You, X.; Lu, W.; Chen, J.; Li, G.; Zhang, L., Label free electrochemical sensor for Pb 2+ based on graphene oxide mediated deposition of silver nanoparticles. *Electrochimica Acta* **2016,** *187*, 286-292.
26. Zhuang, J.; Fu, L.; Xu, M.; Zhou, Q.; Chen, G.; Tang, D., DNAzyme-based magneto-controlled electronic switch for picomolar detection of lead (II) coupling with DNA-based hybridization chain reaction. *Biosensors and Bioelectronics* **2013,** *45*, 52-57.
27. Tang, S.; Tong, P.; Li, H.; Tang, J.; Zhang, L., Ultrasensitive electrochemical detection of Pb 2+ based on rolling circle amplification and quantum dotstagging. *Biosensors and Bioelectronics* **2013,** *42*, 608-611.
28. Seenivasan, R.; Chang, W.-J.; Gunasekaran, S., Highly Sensitive Detection and Removal of Lead Ions in Water Using Cysteine-Functionalized Graphene Oxide/Polypyrrole Nanocomposite Film Electrode. *ACS applied materials & interfaces* **2015,** *7* (29), 15935-15943.
29. Zhang, J.-T.; Jin, Z.-Y.; Li, W.-C.; Dong, W.; Lu, A.-H., Graphene modified carbon nanosheets for electrochemical detection of Pb (II) in water. *Journal of Materials Chemistry A* **2013,** *1* (42), 13139-13145.
30. Gao, C.; Yu, X.-Y.; Xu, R.-X.; Liu, J.-H.; Huang, X.-J., AlOOH-reduced graphene oxide nanocomposites: one-pot hydrothermal synthesis and their enhanced electrochemical activity for heavy metal ions. *ACS applied materials & interfaces* **2012,** *4* (9), 4672-4682.
31. Promphet, N.; Rattanarat, P.; Rangkupan, R.; Chailapakul, O.; Rodthongkum, N., An electrochemical sensor based on graphene/polyaniline/polystyrene nanoporous fibers modified electrode for simultaneous determination of lead and cadmium. *Sensors and Actuators B: Chemical* **2015,** *207*, 526-534.
32. Aragay, G.; Pons, J.; Merkoçi, A., Recent trends in macro-, micro-, and nanomaterial-based tools and strategies for heavy-metal detection. *Chemical reviews* **2011,** *111* (5), 3433-3458.
33. Cai, D.; Song, M., Preparation of fully exfoliated graphite oxide nanoplatelets in organic solvents. *Journal of Materials Chemistry* **2007,** *17* (35), 3678-3680.
34. Gómez-Navarro, C.; Weitz, R. T.; Bittner, A. M.; Scolari, M.; Mews, A.; Burghard, M.; Kern, K., Electronic transport properties of individual chemically reduced graphene oxide sheets. *Nano letters* **2007,** *7* (11), 3499-3503.
35. Wang, X.; Zhi, L.; Müllen, K., Transparent, conductive graphene electrodes for dye-sensitized solar cells. *Nano letters* **2008,** *8* (1), 323-327.
36. Cote, L. J.; Kim, F.; Huang, J., Langmuir− Blodgett assembly of graphite oxide single layers. *Journal of the American Chemical Society* **2008,** *131* (3), 1043-1049.
37. Li, X.; Zhang, G.; Bai, X.; Sun, X.; Wang, X.; Wang, E.; Dai, H., Highly conducting graphene sheets and Langmuir–Blodgett films. *Nature nanotechnology* **2008,** *3* (9), 538-542.

38. Eda, G.; Fanchini, G.; Chhowalla, M., Large-area ultrathin films of reduced graphene oxide as a transparent and flexible electronic material. *Nature nanotechnology* **2008,** *3* (5), 270-274.
39. Mattevi, C.; Eda, G.; Agnoli, S.; Miller, S.; Mkhoyan, K. A.; Celik, O.; Mastrogiovanni, D.; Granozzi, G.; Garfunkel, E.; Chhowalla, M., Evolution of electrical, chemical, and structural properties of transparent and conducting chemically derived graphene thin films. *Advanced Functional Materials* **2009,** *19* (16), 2577-2583.
40. Robinson, J. T.; Zalalutdinov, M.; Baldwin, J. W.; Snow, E. S.; Wei, Z.; Sheehan, P.; Houston, B. H., Wafer-scale reduced graphene oxide films for nanomechanical devices. *Nano letters* **2008,** *8* (10), 3441-3445.
41. Robinson, J. T.; Perkins, F. K.; Snow, E. S.; Wei, Z.; Sheehan, P. E., Reduced graphene oxide molecular sensors. *Nano letters* **2008,** *8* (10), 3137-3140.
42. Pang, S.; Tsao, H. N.; Feng, X.; Müllen, K., Patterned Graphene Electrodes from Solution-Processed Graphite Oxide Films for Organic Field-Effect Transistors. *Advanced Materials* **2009,** *21* (34), 3488-3491.
43. Wang, Z.; Wang, H.; Zhang, Z.; Liu, G., Electrochemical determination of lead and cadmium in rice by a disposable bismuth/electrochemically reduced graphene/ionic liquid composite modified screen-printed electrode. *Sensors and Actuators B: Chemical* **2014,** *199*, 7-14.
44. Jian, J.-M.; Liu, Y.-Y.; Zhang, Y.-L.; Guo, X.-S.; Cai, Q., Fast and sensitive detection of Pb2+ in foods using disposable screen-printed electrode modified by reduced graphene oxide. *Sensors* **2013,** *13* (10), 13063-13075.
45. Wan, H.; Sun, Q.; Li, H.; Sun, F.; Hu, N.; Wang, P., Screen-printed gold electrode with gold nanoparticles modification for simultaneous electrochemical determination of lead and copper. *Sensors and Actuators B: Chemical* **2015,** *209*, 336-342.
46. Kadara, R. O.; Tothill, I. E., Development of disposable bulk-modified screen-printed electrode based on bismuth oxide for stripping chronopotentiometric analysis of lead (II) and cadmium (II) in soil and water samples. *Analytica chimica acta* **2008,** *623* (1), 76-81.
47. Mandil, A.; Idrissi, L.; Amine, A., Stripping voltammetric determination of mercury (II) and lead (II) using screen-printed electrodes modified with gold films, and metal ion preconcentration with thiol-modified magnetic particles. *Microchimica Acta* **2010,** *170* (3-4), 299-305.
48. Choi, S.-J.; Kwon, T.-H.; Im, H.; Moon, D.-I.; Baek, D. J.; Seol, M.-L.; Duarte, J. P.; Choi, Y.-K., A polydimethylsiloxane (PDMS) sponge for the selective absorption of oil from water. *ACS applied materials & interfaces* **2011,** *3* (12), 4552-4556.
49. Bonfil, Y.; Brand, M.; Kirowa-Eisner, E., Characteristics of subtractive anodic stripping voltammetry of Pb and Cd at silver and gold electrodes. *Analytica chimica acta* **2002,** *464* (1), 99-114.
50. Gao, W.; Nyein, H. Y. Y.; Shahpar, Z.; Fahad, H. M.; Chen, K.; Emaminejad, S.; Gao, Y.; Tai, L.-C.; Ota, H.; Wu, E., A Wearable Microsensor Array for Multiplexed Heavy Metal Monitoring of Body Fluids. *ACS Sensors* **2016**.
51. Su, W.; Cho, M.; Nam, J.-D.; Choe, W.-S.; Lee, Y., Highly sensitive electrochemical lead ion sensor harnessing peptide probe molecules on porous gold electrodes. *Biosensors and Bioelectronics* **2013,** *48*, 263-269.
52. Tung, V. C.; Allen, M. J.; Yang, Y.; Kaner, R. B., High-throughput solution processing of large-scale graphene. *Nature nanotechnology* **2009,** *4* (1), 25-29.
53. Brownson, D. A.; Varey, S. A.; Hussain, F.; Haigh, S. J.; Banks, C. E., Electrochemical properties of CVD grown pristine graphene: monolayer-vs. quasi-graphene. *Nanoscale* **2014,** *6* (3), 1607-1621.
54. Behbahani, M.; Hassanlou, P. G.; Amini, M. M.; Omidi, F.; Esrafili, A.; Farzadkia, M.; Bagheri, A., Application of solvent-assisted dispersive solid phase extraction as a new, fast, simple and reliable preconcentration and trace detection of lead and cadmium ions in fruit and water samples. *Food chemistry* **2015,** *187*, 82-88.

55. Pourabadehei, M.; Mulligan, C. N., Selection of an appropriate management strategy for contaminated sediment: A case study at a shallow contaminated harbour in Quebec, Canada. *Environmental Pollution* **2016,** *219*, 846-857.